iScience, Volume *26*

Supplemental information

Bifidobacterium affects antitumor efficacy of oncolytic adenovirus in a mouse model of melanoma

Lorella Tripodi, Sara Feola, Ilaria Granata, Thomas Whalley, Margherita Passariello, Cristian Capasso, Ludovica Coluccino, Maria Vitale, Giulia Scalia, Laura Gentile, Claudia De Lorenzo, Mario Rosario Guarracino, Giuseppe Castaldo, Valeria D'Argenio, Barbara Szomolay, Vincenzo Cerullo, and Lucio Pastore

Table S1. Abundance of phyla obtained by Dunn's test, Related to Figure 4

Treatment	Phylum	Timepoints	Z	Un p-value	Ad p-value
Mock	Tenericutes	-10 to 20	-3.527848	0.00041895	0.00251371
		0 to 20	-2.244994	0.02476849	0.04953698
	Actinobacteria	-10 to 18	-3.3140394	0.00091959	0.00275876
		0 to 18	-3.3674917	0.00075855	0.00455132
Bifidus	Actinobacteria	0 to 20	-3.3140394	0.00091959	0.00551751
	Proteobacteria	-10 to 0	2.7260647	0.00640944	0.03845666
		-10 to 18	2.5657079	0.01029655	0.03088965
	Cyanobacteria	-10 to 0	2.3518989	0.01867785	0.05603355
Ad-CpG	Actinobacteria	-10 to 18	-3.3674916	0.00075855	0.00455132
	Firmicutes	0 to 18	2.6191602	0.00881466	0.02644396
		18 to 20	-3.1002304	0.0019337	0.01160221
Ad-CpG + Bifidus	Actinobacteria	-10 to 18	2.8864214	0.0038965	0.023379
	Firmicutes	-10 to 20	-2.4053512	0.01615693	0.04847079
	Deferribacteres	-10 to 18	2.93987366	0.00328346	0.01970077
		0 to 18	2.88642141	0.0038965	0.0116895
	Cyanobacteria	-10 to 0	2.7805624	0.00542648	0.03255889
		-10 to 18	2.4597283	0.01390422	0.04171267
	Tenericutes	-10 to 18	2.4053512	0.01615693	0.04847079
		0 to 18	2.6726124	0.00752632	0.04515789

Table S1. Results of Dunn's test, applied to the Kruskal-Wallis significant amplicon sequence variants (ASVs) shown in Figure 4 panel A; the phyla shown in the table for each treatment, were obtained from significant comparisons between time pairs, according to the Benjamini and Hochberg's false discovery rate (FDR) correction (BH) adjusted p-value<0.05.

Figure S1. Perturbation of gut microbiome reduced the efficacy of Ad-CpG in a syngeneic mouse model of melanoma, Related to Figure 1

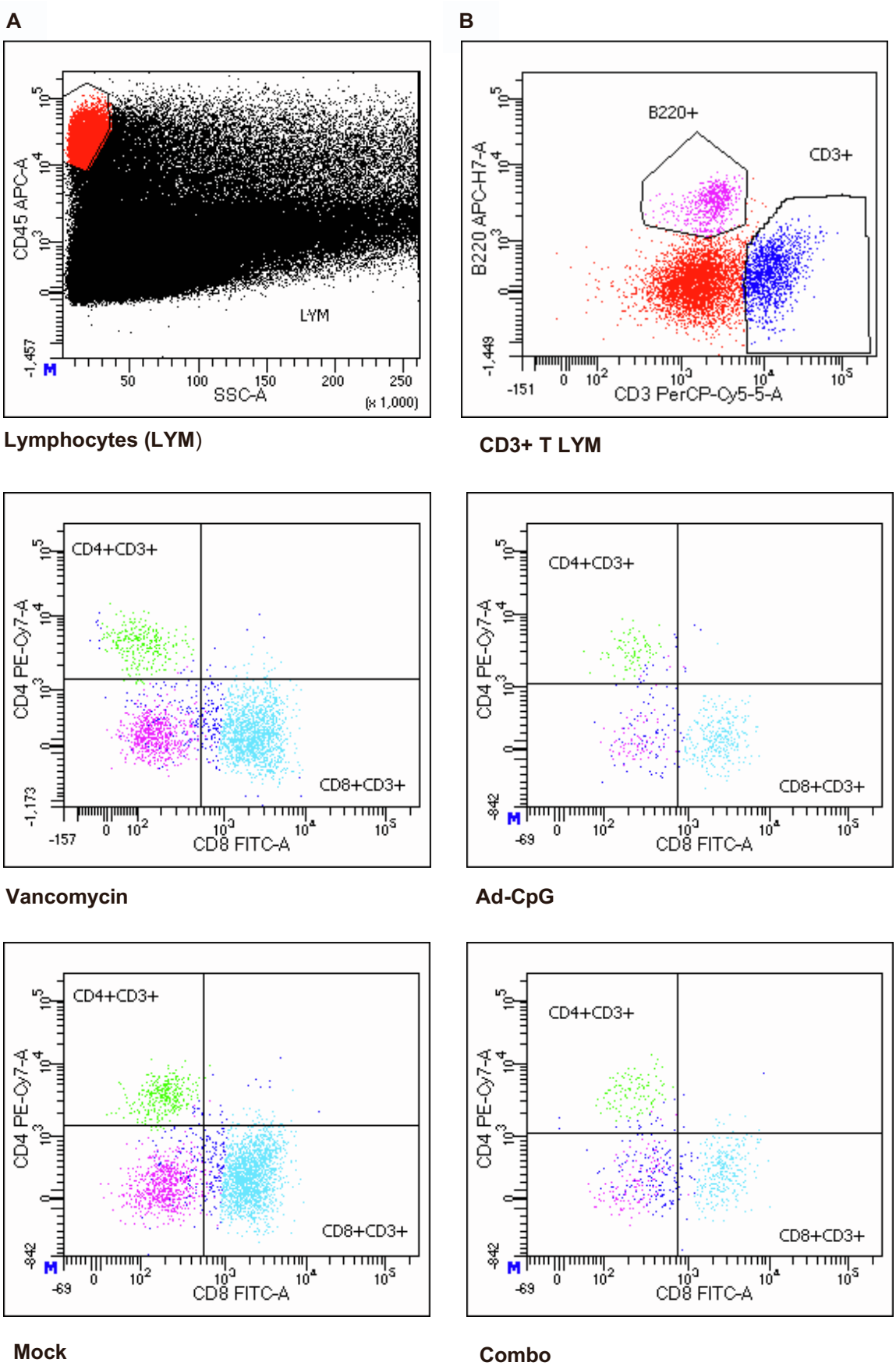

Figure S1. The panel below represents the quadrant gating strategy that has been used for all samples. **A)** The lymphocytes gate was obtained by selecting CD45+ lymphocytes (red color population indicated as LYM) **B)** T lymphocytes CD3+ were gated on CD45+ lymphocytes el). B220 was used to select B lymphocytes among CD45+ lymphocytes. For each treatment, we report the gating strategy of CD8+ CD3+ CD45+ T-lymphocytes and of CD4+ CD3+ CD45+ T lymphocytes.

Figure S2. Flow cytometry representative plots of analysis of Foxp3+ CD4+ CD45+ T lymphocytes collected from Ad-CpG-treated tumors, Related to Figure 3

A

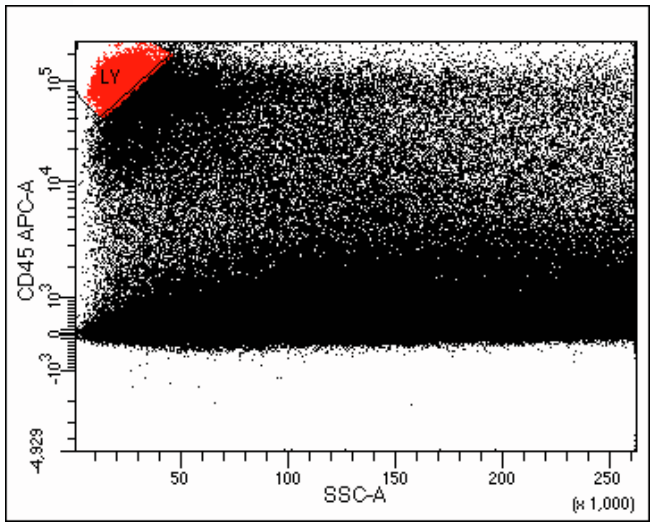

Lymphocytes (LYM)

B

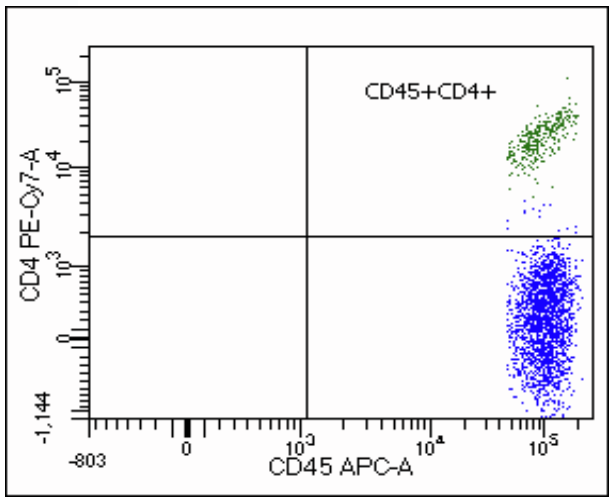

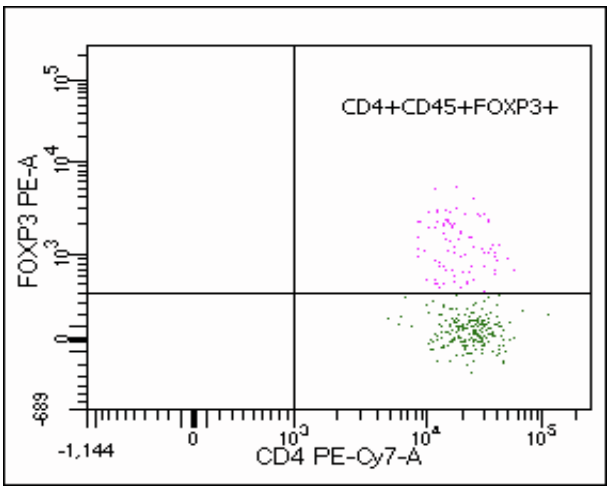

Ad-CpG

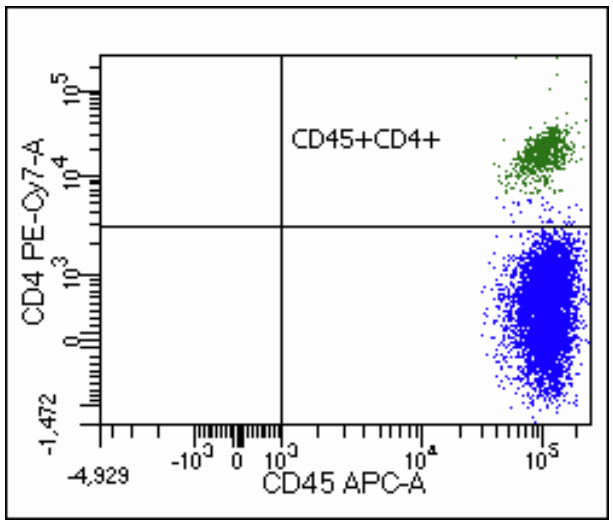

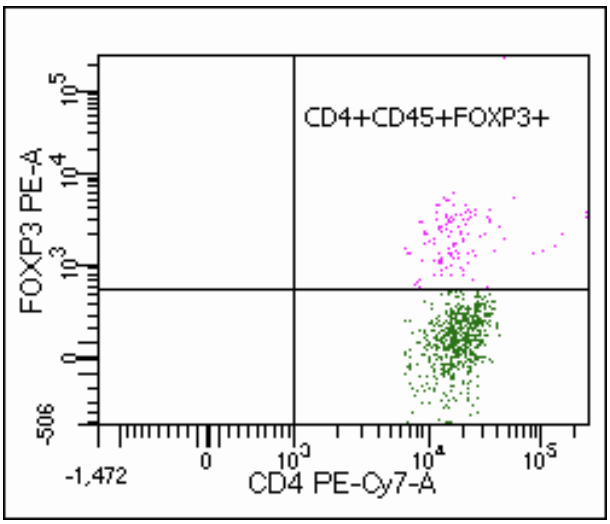

Ad-CpG + Bifidus

Figure S2. The panels represent the quadrant gating strategy that has been used for all tumor samples collected from both OAd- treated mice, indicated as Ad-CpG and Ad-CpG + Bifidus. **A)** Lymphocytes were gated on CD45+ cells. **B)** For each treatment, we report the flow cytometry representative plots of CD4+ CD45+ T-lymphocytes and Foxp3+ CD4+ CD45+ T lymphocytes.

Figure S3. Flow cytometry representative plots of analysis of Foxp3+ CD4+ CD45+ T lymphocytes collected from untreated and Bifidus-treated tumors, Related to Figure 3

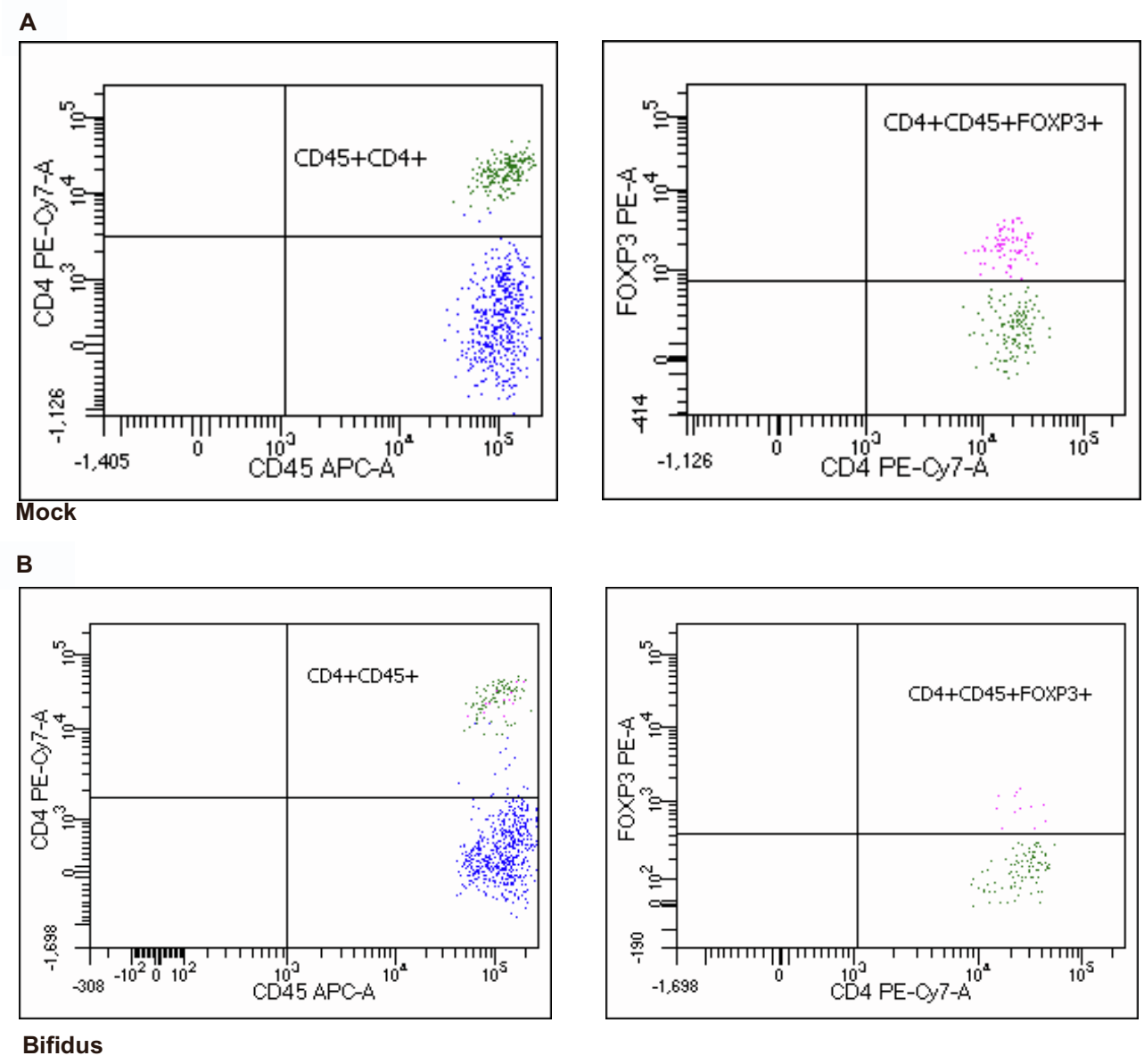

Figure S3. Flow cytometry representative plots of analysis of Foxp3+ CD4+ CD3+ T lymphocytes. **A)** The panels represent the quadrant gating strategy that has been used for all tumor samples collected from untreated mice (Mock) and **B)** from Bifidus-treated group (Bifidus). Lymphocytes were gated on CD45+ cells. For each treatment, we report the flow cytometry representative plots of CD4+ CD45+ T-lymphocytes and Foxp3+ CD4+ CD45+ T lymphocytes.

Figure S4. Flow cytometry representative plots of analysis of Foxp3+ CD4+ CD3+ T lymphocytes collected from Ad-CpG-treated groups, Related to Figure 3

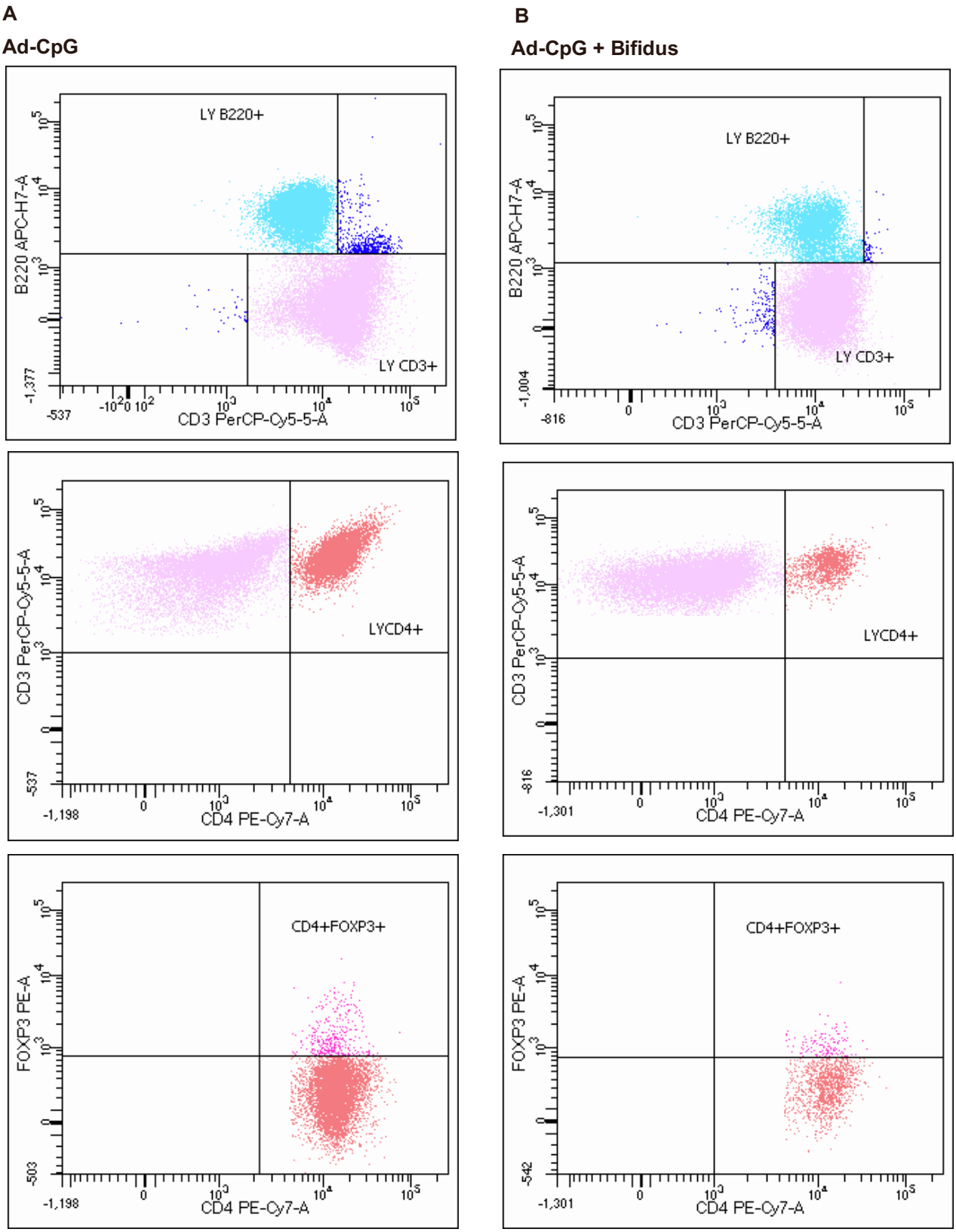

Figure S4. A) The panels represent the quadrant gating strategy that has been used for all spleen samples collected from OAd-treated mice, indicated as Ad-CpG and **B)** from combined regimen-treated mice, indicated as Ad-CpG + Bifidus. B220 was used to select B lymphocytes. For each treatment, we report the flow cytometry representative plots of CD4+CD3+ T lymphocytes and Foxp3+ CD4+ CD3+ T lymphocytes.

Figure S5. Flow cytometry representative plots of analysis of Foxp3+ CD4+ CD3+ T lymphocytes collected from untreated and Bifidus-treated groups, Related to Figure 3

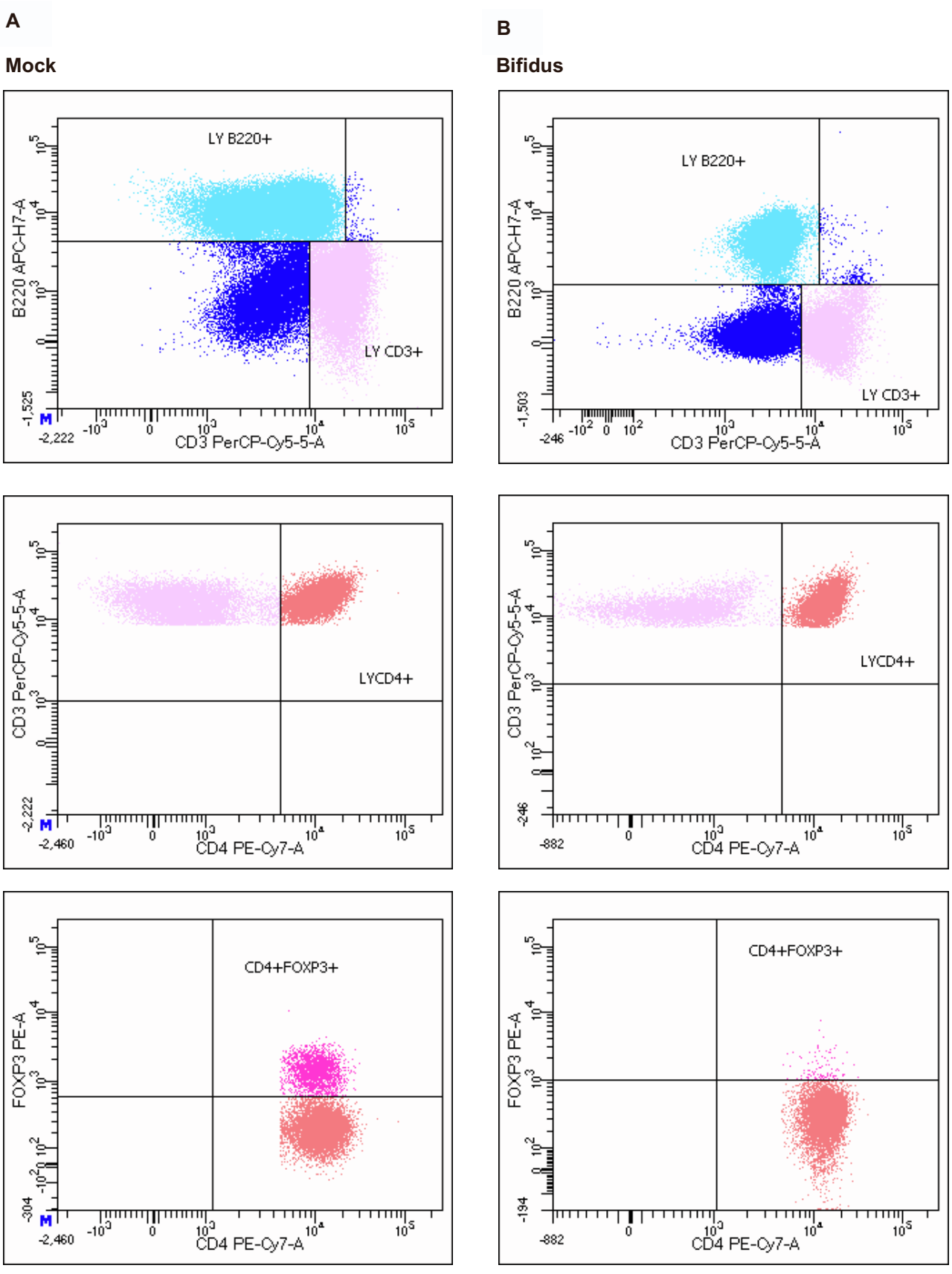

Figure S5. A) The panels represent the quadrant gating strategy that has been used for all spleen samples collected from untreated mice (Mock) **B)** and from Bifidus-treated mice (Bifidus). B220 was used to select B lymphocytes. For each treatment, we report the flow cytometry representative plots of CD4+CD3+ T lymphocytes and Foxp3+ CD4+ CD3+ T lymphocytes.

Figure S6. Co-culture experiment of melanoma cells with splenocytes pre-immunized, Related to Figure 3

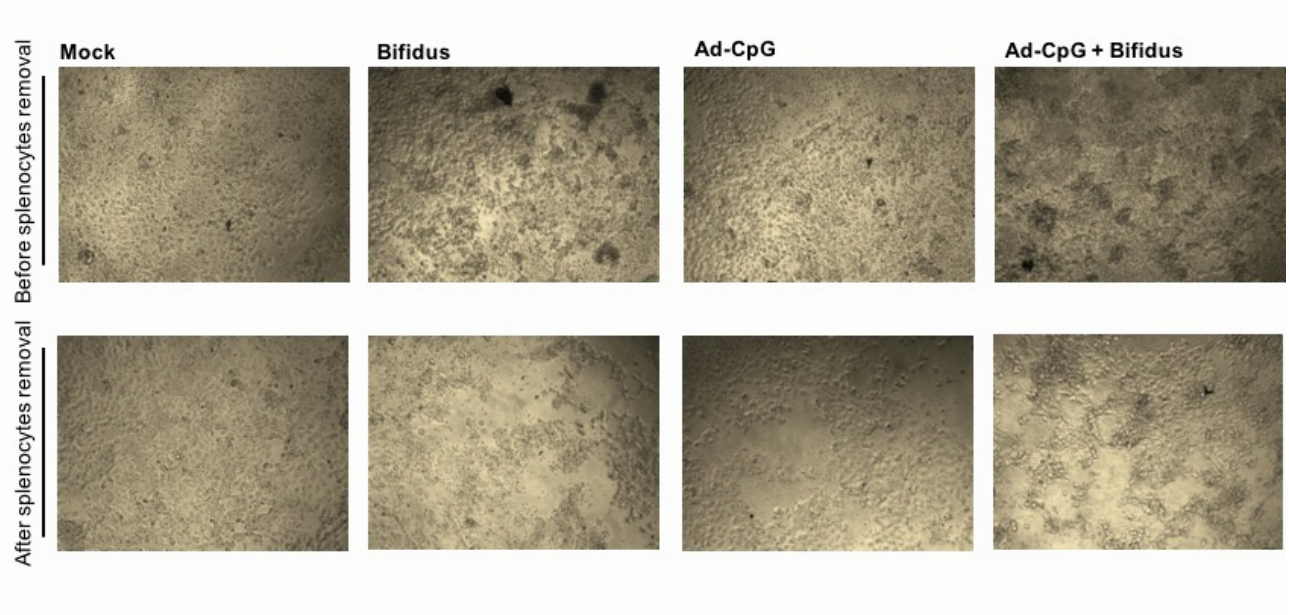

Figure S6. Representative images of B16-OVA cells co-cultured with splenocytes pre-immunized, as indicated (Mock, Bifidus, Ad-CpG and Ad-CpG+Bifidus) were acquired before and after splenocytes removal.

Figure S7. Alpha diversity of microbial communities, Related to Figure 4

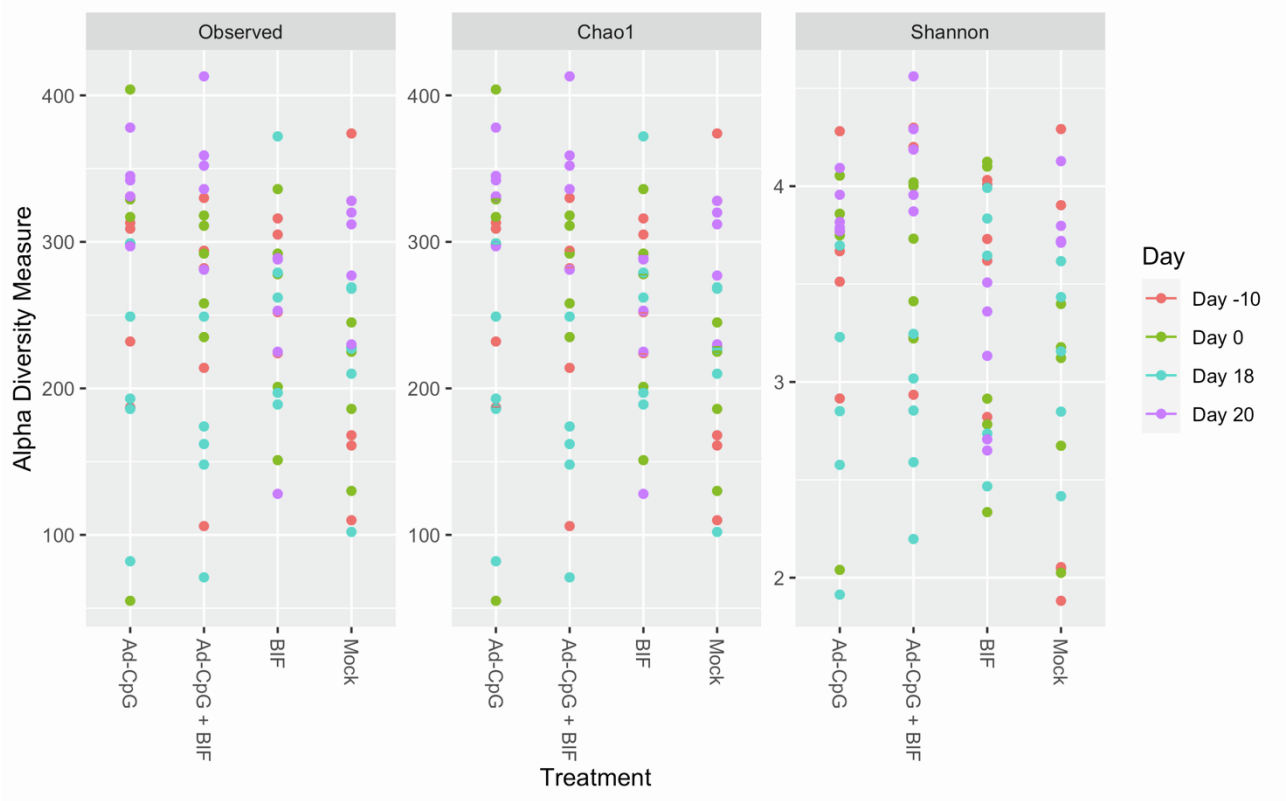

Figure S7. The microbial richness measured by Observed OTU, Chao1 and Shannon indices do not highlight any differences between treatments indicated as: Mock, Bifidus (BIF), Ad-CpG and Ad-CpG+BIF or time points (Day-10; Day 0; Day 18; Day 20)

Figure S8. Beta diversity of microbial communities, Related to Figure 4

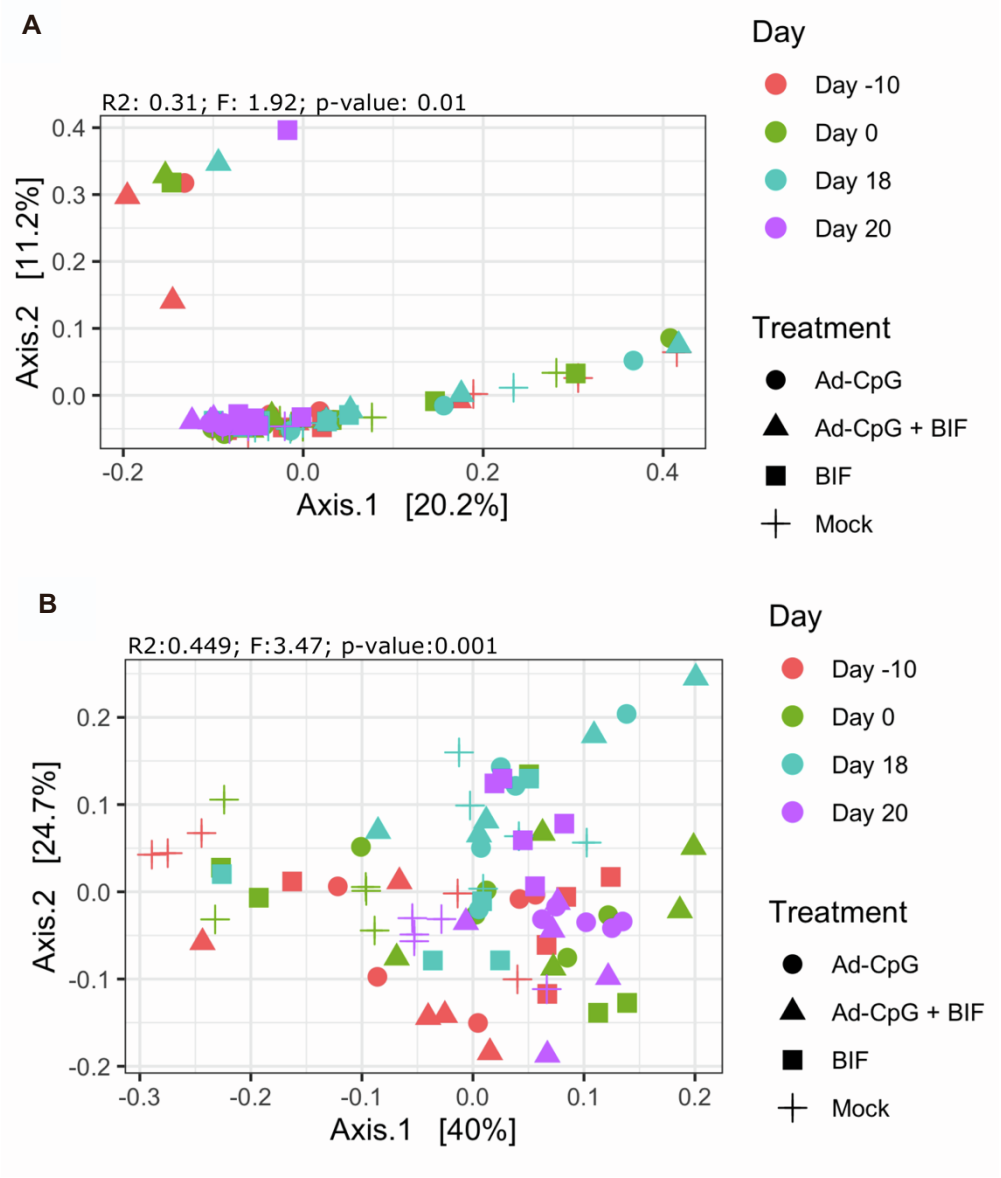

Figure S8. A) Principal coordinates analysis (PCoA) plot of the four groups. The plots show the first two principal coordinates (axes) for PCoA using unweighted UniFrac distances **B)** and weighted UniFrac distances. The treatments are indicated as: Mock, Bifidus (BIF), Ad-CpG and Ad-CpG+BIF and time points as (Day-10; Day 0; Day 18; Day 20). On the top of the plots, the results of *PERMANOVA* statistical test are reported in terms of R2, F statistic and p-value.

Figure S9. Evaluation of immunogenicity of Bifidobacterium-derived peptide B1, and tumor peptides T3 and T4, Related to Figure 7

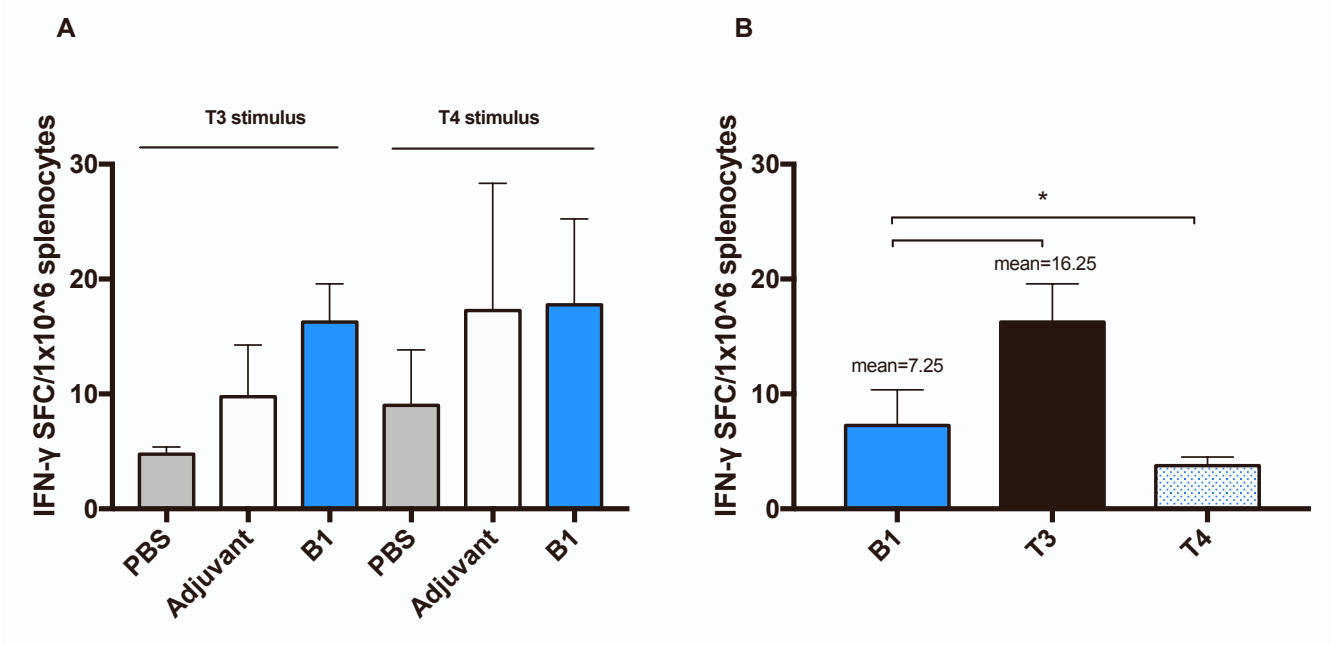

Figure S9. A) IFN-γ ELISpot was performed on harvested splenocytes from mice preimmunized with PBS, adjuvant poly (I:C) and with *Bifidobacterium* peptide B1 and individual response to T3 stimulus and T4 for each group of mice (n=3) is reported as number of spots (IFN-γ). **B)** Comparison of the number of spots IFN-γ detected between splenocytes from mice preimmunized with B1 and pulsed with B1, T3 and T4 stimulus with relative means. All data are depicted as bar plots and mean ± SEM is shown. The statistical analysis was performed with ordinary one-way ANOVA (*p<0.05; **p<0.01; ***p<0.001; ****p<0.0001).